JOURNAL OF AIRCRAFT
Vol. 30, No. 2, March–April 1993

Role of Leading-Edge Vortex Flows in Prop-Fan Interaction Noise

J. C. Simonich,* D. C. McCormick,† and P. L. Lavrich†
United Technologies Research Center, East Hartford, Connecticut 06108

An experimental investigation has been carried out to study the interaction mechanisms associated with wakes from unswept, aft-, and forward-swept vanes incident on rotating prop-fan blades. Wakes from a single, stationary upstream vane interacted with a single rotating prop-fan. Comprehensive flowfield and acoustic measurements were acquired over a range of takeoff operating conditions. The forward-swept vane caused the leading-edge vortex and a core velocity defect associated with it to move inboard towards the hub and away from the high-speed tip region of the prop-fan. The tip vortex had only a small axial velocity disturbance associated with it. This is in contrast to the aft-swept vane which directed the leading-edge vortex out towards the tip, and led a large axial velocity disturbance to be swept toward the prop-fan tip region. Noise measurements revealed that the forward-swept vane wakes generated relatively less interaction noise than the aft-swept vane wakes, at equivalent vane loadings. From this simulation study, a potential noise reduction strategy for the counter-rotating prop-fan is suggested which uses a forward-swept/aft-swept counter-rotating prop-fan combination. By reducing the sweep or modifying the spanwise loading on the blades, it may be possible to control the magnitude and/or location of the velocity defect associated with the leading-edge vortex.

Nomenclature

a = speed of sound
C = vane chord
J = advance ratio, $\pi M_\infty / M_T$
M_T = tip Mach number, $\Omega R_T / a$
M_∞ = freestream Mach number, V_∞ / a
R_T = radius of blade tip
V_A = axial velocity component
V_∞ = freestream velocity
X = axial coordinate
α = vane incidence angle
β = prop-fan blade pitch angle at 75% radius
θ = polar angle relative to upstream
ρ = density
Ω = prop-fan rotational speed

Introduction

THE counter-rotating prop-fan (CRP) radiates noise from a variety of source mechanisms, such as steady loading and thickness noise, but one of the most dominant is that due to aerodynamic interaction. This interaction occurs when the downstream blade responds to wake fluctuations caused by the upstream prop-fan, and is more severe at takeoff conditions. At this high loading condition, one of the major disturbances to the flow into the downstream prop-fan is caused by the leading-edge (LE) vortex shed from the upstream prop-fan blades. This vortex is formed on the suction surface of the prop-fan under high load by flow separating off the sharp leading edge and rolling into a vortex.[1]

A novel experiment has been performed to explore this leading-edge vortex interaction mechanism associated with wakes from swept vanes incident on rotating prop-fan blades. The study was aimed at providing a data base for evaluating and improving noise prediction methodology components, and for enhanced understanding of interaction noise generation.

The counter-rotation geometry was replaced by a simulation study which used a stationary upstream vane to generate prop-fan-like wakes. A single, stationary swept vane (simulating some of the characteristics of a prop-fan) was used to generate a wake upstream of a single rotating prop-fan.

The noise signatures of counter-rotating prop-fans have been shown to be significantly different compared to isolated single prop-fans, mainly because of the interaction of the rotors.[2] This interaction can be substantial (10–15 dB) at a few harmonics above blade passage.[3] For a simulated cruise operating condition, Hanson and Patrick[4] demonstrated that a simple analytical wake theory could effectively explain experimentally observed flow features such as viscous velocity defects, vortex sheets, tip vortices, and propagating acoustic pulses. Tillman and Simonich[5] showed that a small wake deficit caused by the leading-edge vortex exists for cruise conditions. Laser velocimetry data behind a counter-rotating unducted fan at cruise by Podboy and Krupar[6] revealed a slight influence of the potential field upstream of the rotor blades. An experiment on the acoustic tones generated by a model counter-rotating propeller by Nagel and Patrick,[7] established a correlation between the fluctuating components of velocity between the rotors and the interaction noise. They concluded that the circumferential flow was more strongly correlated with the noise than the axial flow.

The current investigation was carried out as part of a test program initially reported in Ref. 8. In that study, a potentially dominant interaction noise source mechanism was identified for the vane wake/prop-fan interaction. The mechanism was related to a velocity defect associated with the leading-edge vortex of the aft-swept vane. The LE vortex, which developed on the aft-swept vane suction surface, was swept radially out towards the vane tip where it was convected downstream into the high-speed tip region of the prop-fan. The resulting vortex defect/blade interaction generated significant blade incidence angle fluctuations, causing unsteady blade loading, which appeared to dominate the noise generation. The vortex structure, including the axial defect, was shown to decay slowly in the streamwise direction, so that almost no noise reduction occurred as the vane/prop-fan distance was increased. Reference 9, using the results of Ref. 8, showed

Presented in parts as Paper 89-1093 at the AIAA 12th Aeroacoustics Conference, San Antonio, TX, April 10–12, 1989 and Paper 90-3977 at the AIAA 13th Aeroacoustics Conference, Tallahassee, FL, Oct. 22–24, 1990; received Nov. 19, 1990; revision received March 20, 1992; accepted for publication March 20, 1992.

*Senior Research Engineer, Aeroacoustics and Experimental Gas Dynamics, M/S 129-17, 411 Silver Lane. Senior Member AIAA.
†Research Engineer, Aeroacoustics and Experimental Gas Dynamics, M/S 129-17, 411 Silver Lane. Member AIAA.

that accurate prediction of prop-fan interaction noise can be made if a reliable description of the ingested wake is available. Another related study by Lavrich et al.[10] examined the wake structure behind a rotating prop-fan at takeoff. A substantial defect in the shed vortex core velocity was found. A model which describes this vortex core velocity distribution was also reported in Ref. 10.

Approach

The vortex interaction mechanisms in an actual counter-rotating prop-fan are very complicated. Several effects such as potential field coupling and aerodynamic interaction occur simultaneously, are interrelated, and cannot be assessed independently. In order to concentrate on the effects of the leading-edge vortex on interaction noise, a simplified program was carried out experimentally. A schematic diagram of the simulation study that was used is shown in Fig. 1. A single stationary vane was placed upstream of the prop-fan to simulate the forward propeller. Three different upstream vane configurations were tested: 1) unswept, 2) aft-swept, and 3) forward-swept vanes.

This experiment was conducted in the United Technologies Research Center (UTRC) acoustic research tunnel, which is an open circuit, open jet design. This facility is described in detail in Ref. 11. All testing was performed at a freestream Mach number of 0.165. The 2-ft-diam prop-fan model consisted of three Hamilton Standard designed CR9 blades and hub, and was powered by an electric motor-drive rig. The swept vanes were held upstream of the prop-fan by a cantilevered nacelle (with the same diameter as the prop-fan hub) which was supported far upstream of the test section. This arrangement assured that only the wake of the vane would interact with the prop-fan and eliminated contaminating effects of support struts or pylons. The upsteam van had 45 deg of sweep, was 5.3% thick, had a 12-in. span and had an 8.485-in. streamwise chord (6-in. chord normal to the leading edge). The vane had a sharp leading edge (0.005-in. radius) and a circular arc profile (in a cross-sectional plane normal to the leading edge), and a half-round tip. This same vane was used for both the aft- and forward-sweep studies. A photograph of the prop-fan drive rig installed in the UTRC acoustic wind tunnel with the aft-swept vane is shown in Fig. 2.

Acoustic measurements were performed using a sideline array of 12, 0.25-in.-diam microphones providing polar directivity angles from $\theta = 23$ to 152 deg relative to upstream. These were located in a common plane at a 20-deg azimuthal angle above a horizontal plane through the tunnel centerline (70 deg from the vane in the direction of prop-fan rotation). This position was selected after preliminary acoustic results indicated the noise to be a maximum at this azimuthal angle.

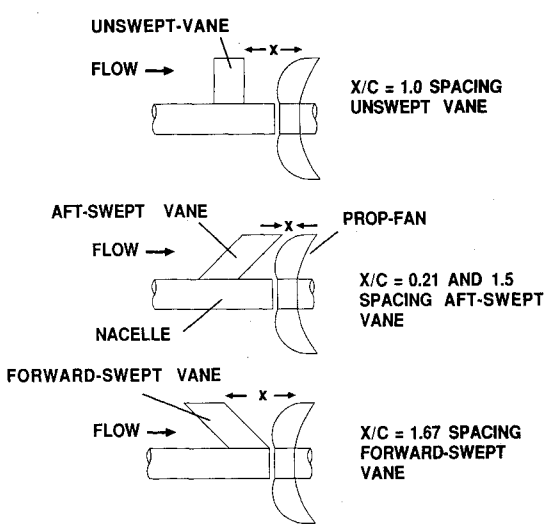

Fig. 1 Counter-rotating prop-fan simulation study.

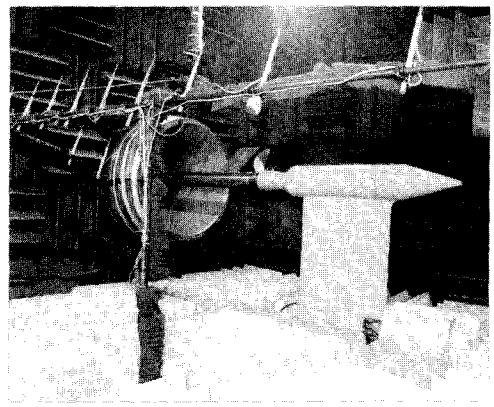

Fig. 2 Prop-fan drive rig installed in UTRC open jet acoustic wind tunnel (note sideline microphone array in foreground).

All wake velocity measurements were taken with a single inclined cylindrical hot film sensor using a multirotation technique which resolves all three velocity components.[10,12] Two flow visualization methods were employed to document different aspects of the flowfield: 1) surface flow visualization using oil flow/tracer, and 2) off surface smoke visualization with both full-field and laser sheet lighting. Details of the acoustic and aerodynamic instrumentation and flow visualization techniques are provided in Ref. 8.

Vane Loading

During the investigation, the vane incidence angle was set at the same value (10- and 20-deg angles of attack) for both the aft- and the forward-sweep configurations. In order to confirm that the vane loading was similar for the two cases, both vane configurations were tested in a low-speed wind tunnel using a lift and drag balance. Although this data was obtained at a lower freestream velocity (60 ft/s), the nondimensional loading coefficients are thought to be representative of the loading for the vanes in the acoustic tunnel test. The results of this test indicated that the aft- and the forward-sweep configurations both yielded very similar lift and drag characteristics for angles of attack below 15 deg. Therefore, valid comparisons of vane wakes can be made at the same incidence angle.

Flowfield

Flow Visualization

The surface streamline patterns for the aft- and forward-swept vanes at angles of attack $\alpha = 10$ and 20 deg are shown in Figs. 3 and 4, respectively. A primary attachment line of the LE vortex is indicated for both angle-of-attack cases for both the aft- and forward-swept vanes. For the forward-swept vane in Fig. 4, the LE vortex originated at the tip and migrated inboard towards the root. This is in contrast to the case of the aft-swept vane shown in Fig. 3 where the LE vortex originated near the blade hub and moved outboard towards the tip. The pattern obtained here is consistent with other forward-swept airfoil investigations (e.g., see Poll and Qiu[13]). The primary attachment line is initially conical and then curves downstream due to the influence of the nacelle. For the 20-deg angle-of-attack case, the LE vortex extends over most of the suction surface inducing a large region of spanwise flow. The presence of a tip vortex for both angles of attack is indicated by the spanwise flow near the tip on both the suction and pressure surfaces. Also, trailing-edge separation with inboard spanwise flow is noticeable on the pressure surface for the 10-deg angle-of-attack case.

Smoke visualization of the flow over the forward-swept vane with full-field illumination is shown in Fig. 5 for a 10-deg angle of attack. To better illustrate the shape of the LE vortex, the video image was enhanced using standard image processing techniques of background subtraction, histogram

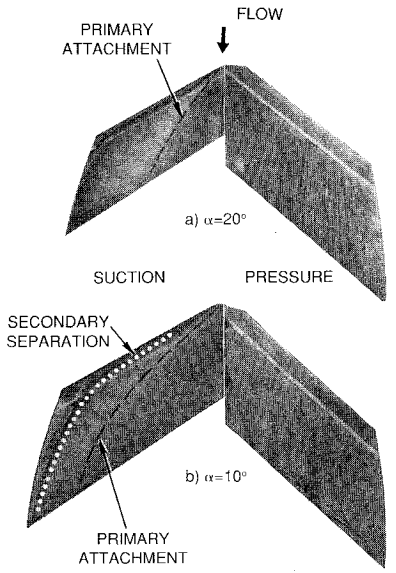

Fig. 3 Surface flow visualization of aft-swept vane.

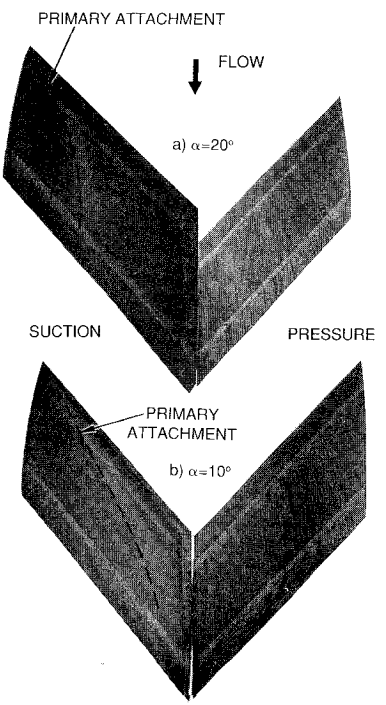

Fig. 4 Surface flow visualization of forward-swept vane (dashed lines indicate LE vortex path).

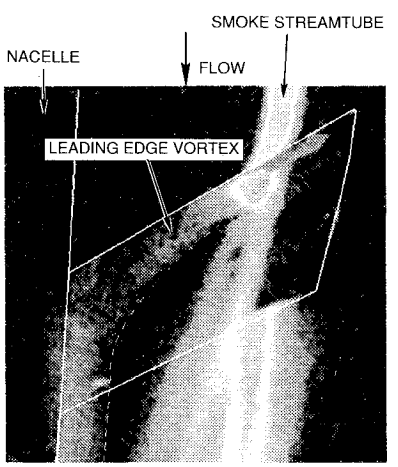

Fig. 5 Enhanced smoke flow visualization of forward-swept vane at 10-deg angle of attack.

equalization and contrast enhancement. It is important to note that variations of the enhancement process do not significantly alter the location of the faired dashed line which represents the spanwise extent of the LE vortex. In the figure, the flow is from top to bottom and the streamtube of smoke intersects the leading edge such that half the smoke passes over the suction surface and half passes over the pressure surface. As can be seen, smoke that is ingested by the LE vortex is pumped spanwise toward the hub. A faired line representing the outboard edge of the smoke has been drawn. The faired line can be seen to closely correspond to the primary attachment line deduced from the surface flow pattern shown in Fig. 4.

The tip vortices shed by the vanes were visualized by smoke flow using laser sheet illumination and are shown in Figs. 6–8 for the aft-swept, unswept, and forward-swept vanes at 10-deg angle of attack. The view shows a cross-sectional slice of the vortices as viewed from downstream looking upstream. For the aft-swept vane in Fig. 6, the tip and LE vortices merge. The result is a vortex with a highly turbulent core structure. The diffuse pattern generated by the smoke is the result of turbulent transport of the smoke through the entire core region.

In contrast, the unswept vane in Fig. 7, which has no LE vortex, and the forward-swept vane in Fig. 8, whose LE vortex is swept inboard, result in clean, well-defined low turbulence tip vortex cores, which appear dark due to the absence of smoke. Although not evident from this view, the LE vortex core on the forward-swept vane has a diffuse nature. Thus, the merging of the LE and tip vortices on the aft-swept vane results in a tip vortex which takes on many characteristics of the LE vortex.

Fig. 6 Laser sheet smoke visualization of tip vortex at $X/C = 2.0$ downstream of the aft-swept vane.

Fig. 7 Laser sheet smoke visualization of tip vortex at $X/C = 1.0$ downstream of the unswept vane.

Fig. 8 Laser sheet smoke visualization of tip vortex at X/C = 1.67 downstream of the forward-swept vane.

Hot Wire Measurements

Velocity measurements behind the vanes were acquired with the prop-fan locked and feathered. It has been previously shown that the effect of propeller induction on the upstream vane flow is negligible for small disk loadings[14] such as the case studied here, so that the measured vane flow should be very similar to the vane flowfield with the prop-fan operating. Hot wire measurements of the three-dimensional flowfield were obtained downstream of the aft- and forward-swept vanes at 10-deg angle of attack. The axial spacing from the trailing edge at the tip location to the measurement plane was 1.5 vane chords for the aft-swept case and 1.96 vane chords for the forward-swept case.

Downstream wake features for the unswept vane model are shown with cross-stream velocity vectors and axial velocity contours in Figs. 9 and 10, respectively. This measurement set was acquired for a fixed vane angle of attack of 6 deg, at a survey plane of X/C = 1.67 downstream of the vane trailing edge. (See Fig. 1 for a definition of the X origin.) For the unswept vane no LE vortex developed, although surface flow visualization showed a small leading-edge separation did occur at this incidence angle. A tip vortex with a small viscous core was observed in the contour plot shown in Fig. 10. A small axial velocity defect was embedded within the vortex core. Peak rotational velocities were $\pm 0.25V_\infty$ with a minimum core velocity of $0.88V_\infty$, which corresponded to the center of the core. Viscous core width was about 3 deg in tangential extent. The vortex was centered about 95% radius.

Figures 11 and 12 show the cross-stream velocity vectors and the axial velocity contours for the aft-swept case. As was seen in the flow visualization experiments, only a single vortex structure exists in the downstream wake. The leading edge and tip vortices, which both have the same sense of rotation, coalesce into a single structure, and are indistinguishable even at this short distance behind the vane. The vortex is centered at a radial position of about 96% radius, and shows noticeable cross stream and axial velocity perturbations from about 80–112% radius, over a tangential angular range of about 14 deg. Peak cross-stream fluctuation velocities vary by $\pm 0.3V_\infty$ around the center of the vortex core. A substantial axial velocity defect ($0.6V_\infty$) also occurs in the center of the vortex core.

The cross-stream velocity vectors and the axial velocity contours for the forward-swept cases are shown in Figs. 13 and 14. For the forward-swept case, the tip and leading-edge vortices are seen as separate structures, with the leading-edge vortex swept in towards the hub. The sense of rotation is different between the two vortices for the forward-swept case. The tip vortex shows peak cross-stream velocities which are nearly the same as the vortex from the aft-swept vane at this same angle of attack as shown in Fig. 11. However, in the forward-swept case, there is little streamwise momentum change

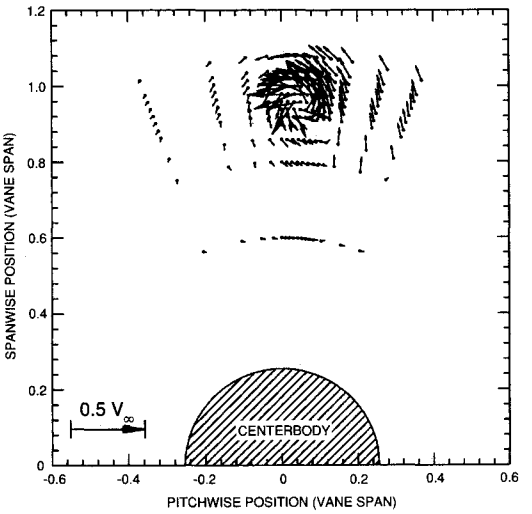

Fig. 9 Cross-stream velocity vectors behind unswept vane at X/C = 1.67 and 6-deg angle of attack.

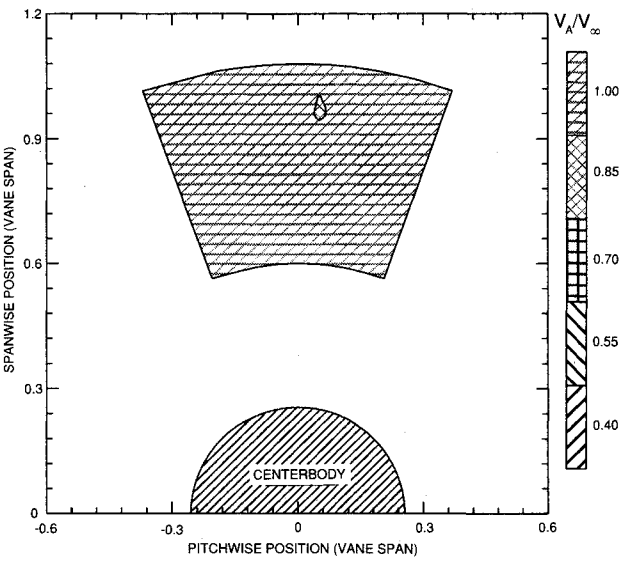

Fig. 10 Streamwise velocity contours behind unswept vane at X/C = 1.67 and 6-deg angle of attack.

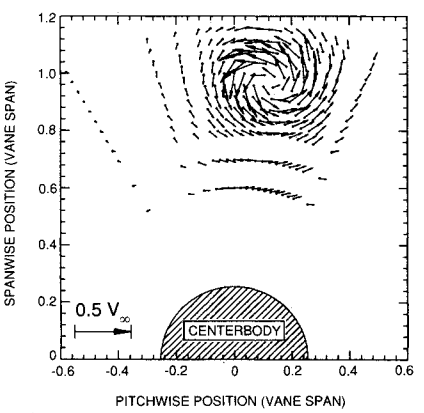

Fig. 11 Cross-stream velocity vectors behind aft-swept vane at X/C = 1.5 and 10-deg angle of attack.

(no axial velocity defect) associated with the tip vortex. The tip vortex structure in this instance is more compact than in the aft-swept case. Substantial changes in tangential and radial velocities are confined between about 88–106% radius with a tangential extent of about 6 deg. The LE vortex for the forward-swept case is driven towards the hub (centerbody). The cross-stream velocity components are substantially less in this structure than those associated with the tip vortex.

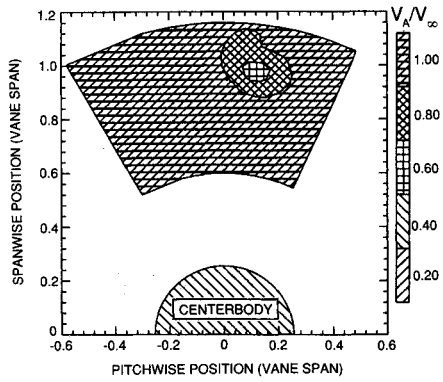

Fig. 12 Streamwise velocity contours behind aft-swept vane at X/C = 1.5 and 10-deg angle of attack.

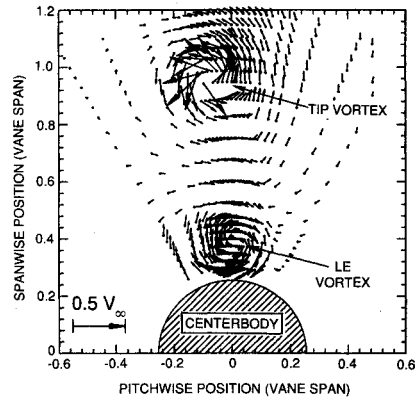

Fig. 13 Cross-stream velocity vectors behind forward-swept vane at X/C = 1.96 and 10-deg angle of attack.

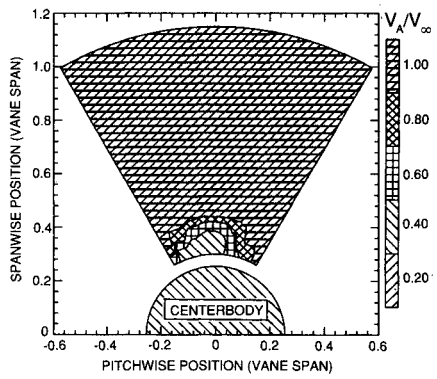

Fig. 14 Streamwise velocity contours behind forward-swept vane at X/C = 1.96 and 10-deg angle of attack.

Rotational velocities are roughly $\pm 0.15V_\infty$. However, there is a large core axial velocity defect observed. This defect is as large as 70% of the freestream axial velocity (V_A/V_∞ = 0.30); this is somewhat larger than that seen in the aft-swept vortex. This vortex is also quite large in extent, extending from the hub (26% radius) to about 44% radius. The tangential extent of the core is roughly 30 deg (equivalent to about 10 deg at the tip).

Note that the structure of the vortex from the forward-swept vane is somewhat different than that from the aft-swept vane; corresponding to a solid body type rotation with the largest rotational velocities near the outer edge of the vortex. The solid body rotation core in the leading-edge vortex extends almost to the edge of the vortex. In contrast, the tip vortex has peak rotational velocities near the core of the vortex, resembling a potential vortex much more.

In summary, the hot wire measurements confirm and quantify the tip and LE vortex structures observed in the flow visualization. For the aft-swept case, the LE and tip vortices are merged, even very close to the airfoil tip, which results in a large, turbulent vortex core with a substantial axial defect.

In contrast, for the forward-swept vane at equivalent loading, the LE and tip vortices are segregated with the LE vortex driven inboard to the hub. The tip vortex in this case is more compact, with a well defined, low turbulence vortex core, with little axial velocity deviation from the freestream. The LE vortex, however, has a large solid body rotation core, is highly turbulent, and causes a very large reduction in axial velocity.

Interaction Noise

A comparison of a typical enhanced frequency spectrum for the baseline case of the prop-fan alone and an interaction noise configuration using the swept vane with the prop-fan at the same operating condition, J = 0.785, β = 31 deg, is shown in Fig. 15. The baseline case shows the classical blade loading spectrum with the blade passage frequency (BPF) harmonics decreasing nearly linearly (in dB) with increasing frequency. The BPF harmonics disappear into the facility background noise beyond the eighth discrete tone. The interaction case has nearly identical first and second harmonics as the baseline test condition, but higher harmonics contain more energy.

In order to present a parameter which represents a measure of the overall interaction sound level for the vane/prop-fan system, an interaction noise metric was formulated. Since the first few harmonics of blade passage frequency are dominated by steady loading noise, they were eliminated from the metric. Harmonics greater than about eight were lost in background noise. The metric chosen was an overall sound power level for all the microphone locations over the 3rd through the 7th harmonics. The choice of this metric was somewhat arbitrary, but should give a useful indication of interaction noise strength. The metric was computed after the noise data had been corrected for shear layer refraction[15] and converted to a common distance.

Figure 16 shows the effect of forward and aft sweep on the interactive sound power metric as a function of advance ratio (and hence blade loading) for a 31-deg prop-fan blade pitch angle. In each instance, the baseline prop-fan alone noise without any upstream vane was subtracted from the measured metric so that 0 dB corresponds to the noise of the rotor alone.

The wake from the forward-swept vane has a dramatic effect on interaction noise levels over the entire range of ad-

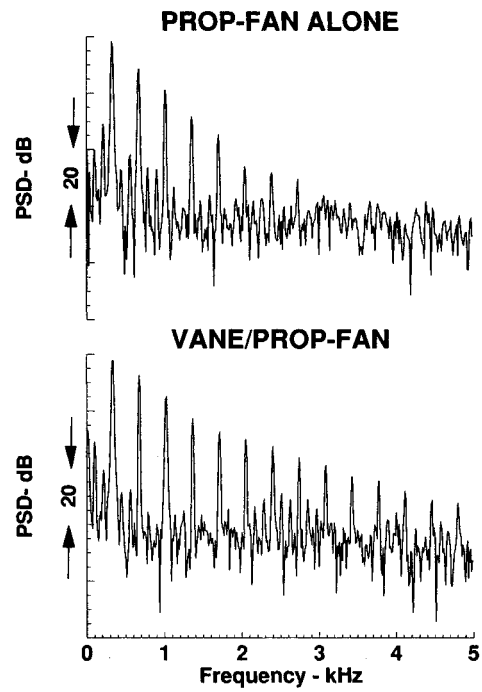

Fig. 15 Comparison of spectrum between prop-fan alone and vane/prop-fan combination (J = 0.785, β = 31 deg).

vance ratios tested. The forward-swept vane wake case is slightly louder than the straight vane case and quieter than the aft-swept vane wake by as much as 10 dB for high advance ratios. The reason for the decreased noise was traced to the location of a defect in axial velocity associated with the leading-edge vortex. The downstream prop-fan experiences a periodic airflow due to the axial velocity defect associated with the LE vortex. This produces a fluctuating angle of attack on the downstream prop-fan blade which in turn causes the blade to experience a fluctuating pressure field, which is the noise generation mechanism. For low relative blade flow angles which are of interest here, the incidence angle is much more sensitive to variations in axial velocity than tangential velocity. For the aft-swept vane, the LE vortex and its associated vortex core defect are driven out to the high-speed tip region of the prop-fan. In contrast, for the forward-swept vane, the LE vortex is propelled inboard toward the relatively low-speed hub and away from the tip.

Acoustic data was also examined in the time domain. Figure 17 shows the time signatures that have been synchronously averaged 200 times for an advance ratio of $J = 0.785$. Five different interaction cases are shown: 1) prop-fan alone, 2) unswept vane ($X/C = 1.67$), 3) forward sweep ($X/C = 1.96$), 4) aft-sweep with close spacing ($X/C = 0.21$), and 5) aft-sweep with far spacing ($X/C = 1.5$). The signatures for six different polar microphone angles (0 deg referenced to upstream) are shown.

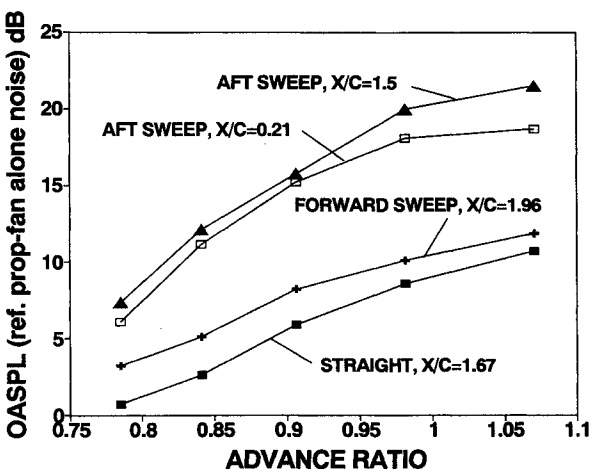

Fig. 16 Effect of sweep orientation on overall sound power level for 31-deg prop-fan blade angle.

Two different axial spacing cases, $X/C = 0.21$ and $X/C = 1.5$, are shown for the aft-swept configuration in Figs. 16 and 17. The effect of changing the axial spacing between vane and prop-fan is seen to be small for the aft-swept case. The noise levels did not change appreciably since the vortical wakes did not dissipate rapidly in the axial direction. Even though the tip of the vane was further upstream for the forward swept case, it is not expected that the decrease in noise observed for this case is due to vortex decay.

For all of the signatures in Fig. 17 there appears to be very little blade-to-blade variation, indicating that the blades were geometrically similar and set at the same blade pitch angle. For the baseline prop-fan alone case, the signatures appear to have the classical blade loading sinusoidal characteristic. On the other hand, both of the aft-swept cases are more impulsive in character with sharper peaks and valleys. Ripples in the waveform, particulary at low polar angles, correspond to higher harmonic content above the blade passage frequency. The forward-sweep case, however, appears to share more of the characteristics of the baseline case than the aft-sweep case. This case does have some ripple in the valleys which are not present in the baseline at the $\theta = 98.5$ and 118.5 deg microphone positions. Additional data not shown here confirms that there is very little change in the shape of the signatures for a moderate variation in advance ratio. Only the amplitudes are different.

Interaction Noise Mechanism

This section discusses the phenomena controlling the vane wake/prop-fan interaction noise mechanism. The LE vortex, developed on the vane suction surface, was swept radially towards the vane tip region where it was convected downstream into the high-speed tip region of the prop-fan. It is assumed that the resulting vortex velocity defect/blade inter-

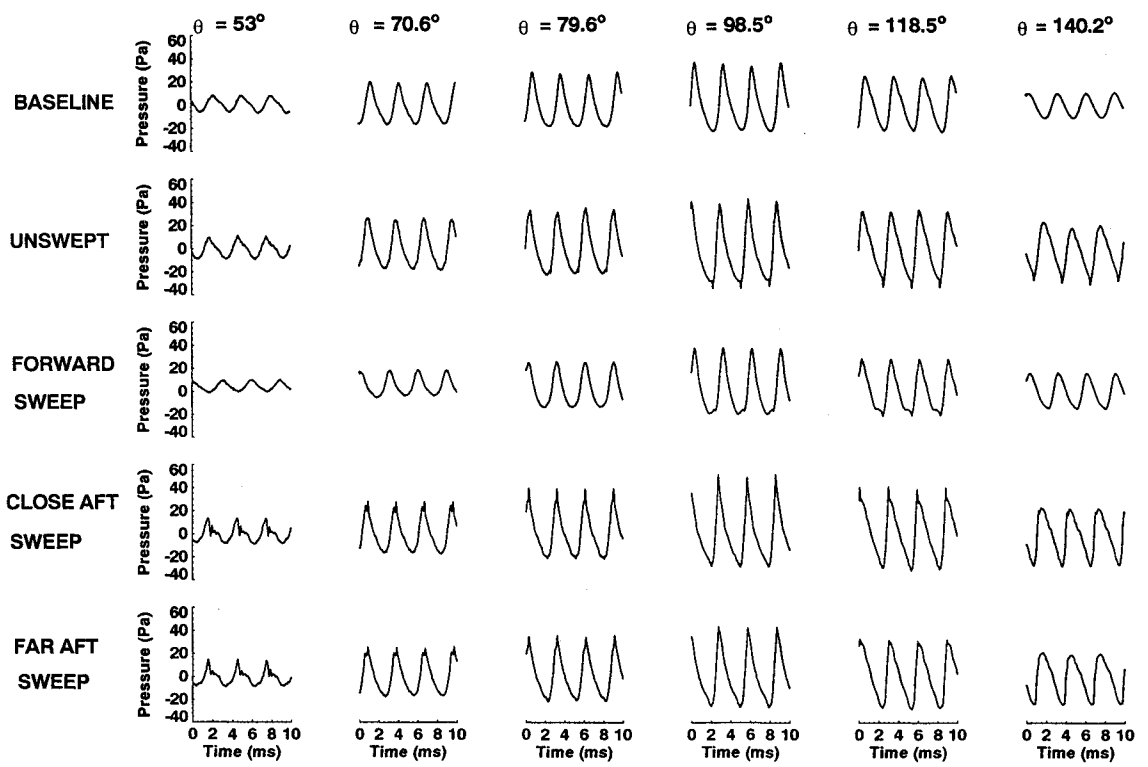

Fig. 17 Pressure waveforms for five different interaction cases, $\beta = 31$ deg, $J = 0.785$.

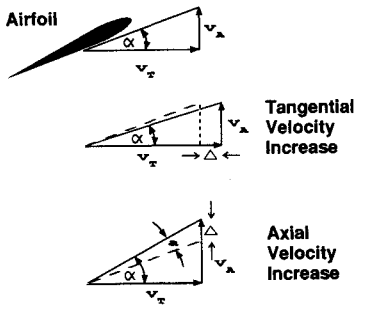

Fig. 18 Effect of axial velocity on unsteady lift.

action generated significant blade surface pressure fluctuations which appeared to dominate the interaction noise generation.

The orientation of the incident wake velocity fluctuations at the prop-fan blade leading edge is critical to the noise level. The important velocity component can be shown to be the axial change associated with the fixed vane defect. This is evident from Fig. 18 which shows schematically how a change in axial velocity V_A and tangential velocity V_T alter the prop-fan flowfield incidence angle. For the vane wake measurements reported above, changes in tangential velocity have little effect on the downstream blade incidence angle α. In contrast, fluctuations in axial velocity of the same magnitude produce a larger change in incidence angle, and hence increased noise. Therefore, it is assumed that the trailing vortex wake defect, rather than the vortex swirling velocity field, is the dominant noise mechanism in the current study.

Although the trailing vortex wake defect was identified as an important contribution to the interaction noise for the fixed vane wake study, only a single aspect of the interaction noise mechanism in CRP systems is modeled. The actual prop-fan interaction may be substantially different, since the wake impingement orientation will be different.

It appears likely that introducing forward sweep to the front prop-fan of a counter-rotating pair may substantially reduce interaction noise and represents a potential noise reduction strategy. There are, however, unknown effects which rotation and vortex intersection geometry will introduce.

Summary

For the aft-swept fixed vane case (simulating the current generation of prop-fan blades), the LE vortex develops on the suction surface and is swept out towards the tip, which is a high velocity region for the trailing blade row. The opposite occurs for the forward-swept vane. The LE vortex and its associated axial velocity defect is pushed down towards the hub and away from the high-speed tip region of the trailing blade row. Noise measurements revealed that forward-swept vane wakes generate relatively less interaction noise than the aft-swept vane wakes at the same vane loading. The forward-swept vane pressure waveform is also less impulsive than the waveform for the aft-swept vane.

From this simulation study, a potential noise reduction strategy which uses forward sweep for the first blade row of the counter-rotating prop-fan was identified. However, in an actual counter-rotating prop-fan, the effects demonstrated in this study may well be different due to the different vortex/blade intersection geometries and the effect of centrifugal force on the LE vortex trajectory. By reducing the sweep or modifying the spanwise loading on the blades, it may be possible to control the magnitude and/or location of the velocity defect associated with the LE vortex.

Acknowledgments

The technical and financial support for this study was given by United Technologies Research Center, Pratt and Whitney Division, and Hamilton Standard Division of United Technologies Corporation. Program supervision was provided by R. H. Schlinker. The authors gratefully acknowledge the support given by B. Magliozzi, and D. Hanson of Hamilton Standard, and J. McCann of Pratt and Whitney.

References

[1]Vaczy, C. M., and McCormick, D. C., "A Study of the Leading Edge Vortex and Tip Vortex on Prop-Fan Blades," *Journal of Turbomachinery*, Vol. 109, July 1987, pp. 325–331.

[2]Magliozzi, B., "Advanced Turboprop Noise, a Historical Review," AIAA Paper 84-2261, Oct. 1984.

[3]Magliozzi, B., "Noise Characteristics of a Model Counter-Rotating Prop-Fan," AIAA Paper 87-2656, Oct. 1987.

[4]Hanson, D. B., and Patrick, W. P., "Near Wakes of Advanced Turbopropellers, AIAA Paper 89-1095, April 1989.

[5]Tillman, T. G., and Simonich, J. C., "Hot Wire Measurements Downstream of a Prop-Fan," *Journal of Propulsion and Power*, Vol. 7, No. 5, 1991, pp. 776–783.

[6]Podboy, G. G., and Krupar, M. J., "Laser Velocimeter Measurements of the Flowfield Generated by an Advanced Counterrotating Propeller," AIAA Paper 89-0434, Jan. 1989; see also NASA TM-101437.

[7]Nagel, R. T., and Patrick, H. V. L., "Aerodynamic Interaction Tones of a Model Counter-Rotating Propeller," *AIAA Journal*, Vol. 26, No. 3, 1988, pp. 498–500.

[8]Simonich, J., McCormick, D., and Lavrich, P., "Interaction Noise Mechanisms for Advanced Propellers—Experimental Results," AIAA Paper 89-1093, April 1989.

[9]Parzych, D., and Lavrich, P., "Interaction Noise Mechanisms for Advance Propellers—Analytical Evaluation," AIAA Paper 89-1094, April 1989.

[10]Lavrich, P. L., McCormick, D. C., and Parzych, D. J., "Vortex Structure of Wakes Behind an Advanced Propeller at Takeoff Load Conditions," AIAA Paper 90-3978, Oct. 1990.

[11]Paterson, R. W., Vogt, P. G., and Foley, W. M., "Design and Development of the United Aircraft Research Laboratories Acoustic Research Tunnel," *Journal of Aircraft*, Vol. 10, No. 7, 1973, pp. 427–433.

[12]Lavrich, P. L., "Time Resolved Measurements of Rotating Stall in Axial Flow Compressors," MIT Gas Turbine Labs., GTL Rept. 194, Cambridge, MA, Aug. 1988.

[13]Poll, D. I. A., and Qiu, C., "A Comparison of the Aerodynamic Characteristics of Swept Forward and Swept Back Wings, *Proceedings of International Conference on Forward Swept Wing Aircraft*, Bristol, England, UK, Sessions I, March 1982, pp. 20.1–20.15.

[14]Horne, W. C., and Soderman, P. T., "Flow-Field Survey of an Empennage Wake Interacting with a Pusher Propeller," NASA-TM-101003, Oct. 1988.

[15]Amiet, R. K., "Refraction of Sound by a Shear Layer," AIAA Paper 77-54, Jan. 1977.